

# Deep Reinforcement Learning for Distributed Uncoordinated Cognitive Radios Resource Allocation

Ankita Tondwalkar and Andres Kwasinski

Rochester Institute of Technology, Rochester, New York 14623, USA  
 {at3235, axkeec}@rit.edu

**Abstract**— This paper presents a novel deep reinforcement learning-based resource allocation technique for the multi-agent environment presented by a cognitive radio network that coexists through underlay dynamic spectrum access (DSA) with a primary network. The resource allocation technique presented in this work is distributed, not requiring coordination with other agents. By ensuring convergence to equilibrium policies almost surely, the presented novel technique succeeds in addressing the challenge of a non-stationary multi-agent environment that results from the dynamic interaction between radios through the shared wireless environment. Simulation results show that in a finite learning time the presented technique is able to find policies that yield performance within 3 % of an exhaustive search solution, finding the optimal policy in nearly 70 % of cases, and that standard single-agent deep reinforcement learning may not achieve convergence when used in a non-coordinated, coupled multi-radio scenario.

## I. INTRODUCTION

The ever increasing resources needs from wireless networks has lead to an understanding of the need for more efficient and effective approaches to the use of the radio spectrum based on shared access through what is known as Dynamic Spectrum Access (DSA). At the same time, cognitive radios (CRs) are considered as the answer to realize the promise of DSA through their ability to autonomously gain awareness of the wireless network environment and learn to adapt to changing conditions by applying machine learning technology. Because of its model-free characteristic, reinforcement learning (RL) is the machine learning approach to resource allocation that naturally aligns with this vision for CRs. However, the application of RL in general wireless networking scenarios present the challenge that the multiple CR links are entangled through the shared spectrum, materialized by the actions of one CR (its transmissions) affecting the environment (e.g. interference) of the other CRs, and resulting in a multi-agent non-stationary environment.

In this work we consider a CR network (CRN) that operates by sharing the network with a primary network (PN), incumbent to the used radio spectrum band, by following an underlay DSA paradigm. In the underlay DSA paradigm, a secondary network (SN) composed of CRs, share the spectrum with a PN by transmitting at power levels such that the interference created on the PN is maintained below a limit. Furthermore, based on practical considerations, we assume that the PN and the SN share the spectrum without exchanging any information with each other. The goal of this work is to develop a RL mechanism for the CRs in the SN to autonomously and independently learn each of their optimal transmit power setting. As such, we also impose the conditions that the CRs cannot exchange coordinate with each other during the RL process (through, for example, exchanging information about actions being taken). This setting belongs to a class of no-

toriously challenging RL problems known as Weakly Acyclic Stochastic Dynamic Games for which there was no known RL algorithm with guaranteed convergence to the optimal policy. However, [1] recently presented a modified general table-based Q-learning algorithm (a very common form of RL) for which almost sure convergence in an asymptotic infinite learning time was proved.

At the same time, the research area of RL have seen notable advances over the recent past years. The works [2], [3] by Mnih, Silver and colleagues constitutes a major milestone by introducing the deep Q-networks (DQNs), a new approach to Q-learning based on the use of deep neural networks approximate the Q action-value function. These works showed the much better learning performance of DQNs compared to standard table-based Q-learning by exhibiting superhuman performance in single-agent at playing Go and video games. This advance spurred research into the application of single-agent DQNs for a variety of applications, including wireless communications. In [4], a power control method single agent Deep Q-learning (DQL) technique was introduced for an underlay CR system consisting of a single primary link and a single secondary. Also, the work [5] applied DQL for scheduling in the Internet-of-Things, [6] applied DQL to dynamic resource allocation in cloud Radio Access Networks, [7] studied the application of DQL to control interference alignment, and the work in [8] use DQL as a trainable function approximator for arbitrary resource allocation algorithms.

The main contribution of this paper is to present a multi-agent DQL technique for distributed resource allocation in a CRN with no requirement for agents coordination. The key challenge addressed by our technique is that the presence of multiple active learning CR leads to a non-stationary environment due to the interaction of the learners through the shared wireless environment. To the best of our knowledge, ours is the first work to present a multi-agent DQL technique for distributed CR resource allocation that converges to the optimal policy almost surely as learning time tends to infinity despite that uncoordinated interaction of the agents leads to a non-stationary environment. The field of works researching multi-agent DQL for wireless communications is rapidly growing but still sparse and, in contrast to our proposed technique, have focused on scenarios that do not present a non-stationary environment because of allowing agent coordination or learning at a central node. In this regards, [9] presents a power allocation technique for a cellular network using DQL based on training a DQN at a central node. The work in [10] also presents a DQN technique with centralized training based on the experiences gathered by the all agents, making the RL solution being more akin to a distributed single agent system rather than a dynamic multi-agent case.

While our proposed DQL technique can achieve convergence to optimality with learning time tending to infinity, we will show through simulation results that in a finite learning time our technique reaches the optimal policy in nearly 70 % of cases and yields an overall mean performance within 3 % of the exhaustive search optimal solution. Moreover, as a second key contribution of this work, we present a case that shows that the application of standard single-agent DQL in uncoordinated distributed CR resource allocation may not reach convergence (to any policy, optimal or not) due to the large noise present in Q-value estimation from the non-stationary environment.

## II. SYSTEM SETUP AND PROBLEM FORMULATION

In this work we will consider a system comprised of two networks that operate by sharing the same radio spectrum band following an underlay DSA mechanism. In the system, a primary network (PN) is incumbent to the spectrum band in use and a secondary network (SN) is formed by CR which are assumed to operate in a fully autonomous manner, i.e. there is no coordination between the CR nodes during resource allocation and no exchange of information whatsoever between both the wireless networks. Following underlay DSA operation, the CRs in the SN are limited in their transmit power so that the interference they create on the PN does not exceed an established limit.

The primary network is comprised of  $M$  access points (APs) transmitting to wireless devices. Over the spectrum band of interest, each AP communicates with one wireless receiver. All transmissions in the PN utilize adaptive modulation and coding (AMC) to control the modulation scheme and channel coding rate on the link based on the experienced Signal-to-Interference-plus-Noise ratio (SINR). We assume that the APs in the PN set their transmit power following the iterative power allocation algorithm in [11].

To operate following underlay DSA, we assume that each CR is able to assess the effect of its transmission on the PN by estimating the relative change (reduction) in the throughput at its PN link. The estimation of relative throughput change is correlated with the interference that the CR is creating on its nearest PN link and presents the advantage that it can be estimated by a CR without any exchange of information between the PN and SN, [12]. As such, owing to the equivalence between SINR and relative throughput change, the CRs implement underlay DSA by monitoring and avoiding to exceed a limit on the relative throughput change in their nearest PN link. As matter of clarification, we note that throughout this paper the “nearest” link is understood to be the one that is received with largest signal power.

As customary, nodes in both wireless networks perform resource (power in this work) allocation in order to optimize their transmission. In the case of CRs, increasing transmit power will increase throughput but will also increase the relative throughput change at its nearest PN link, risking to exceed the underlay DSA-imposed limit. Therefore, we seek an algorithm for each transmitting CR to find its transmit power such that it achieves the largest possible throughput without exceeding the limit on relative throughput change on its nearest PN link. Moreover, for the algorithm to be applicable when there is no coordination between the CRs and no exchange of information between the PN and SN.

## III. DQN-BASED DISTRIBUTED AND UNCOORDINATED MULTI-AGENT RESOURCE ALLOCATION

Because of enabling model free learning of transmission parameters, in this work we adopt the use of RL in the form of Q-learning to solve the CR resource allocation problem described in the previous section. The common principle to RL techniques is that a learning agent is able to find a resource allocation policy by following an iterative procedure of trying out multiple times each available action and using an received instantaneous realization of a reward to estimate the expected discounted reward for each possible action. Specifically, let  $X = \{x_1, x_2, \dots, x_n\}$  be the set of environment states, and  $A = \{a_1, a_2, \dots, a_m\}$  be the set of actions. At time  $t$ , the agent takes an action  $a(t) \in A$  on the environment while it is in state  $x_t \in X$ . During this interaction with the environment, the agent achieves an immediate reward  $r(x, a)$  and the system transitions into a new state  $x_{t+1} \in X$ . A reward function represents the effect of selected action on the environment. The same set of actions as well as states are assumed for all SUs. We define the state space, action space and reward function of the DQN-based learning framework as follow:

**Action space:** Each CR will search over the discrete action space  $A = \{0, p_0, p_1, \dots, p_L\}$  of possible transmit powers (with a setting of '0' indicating no transmission), for the best choice that maximizes throughput while meeting the underlay DSA constraint (limit on relative throughput change on a PN link).

**State space:** The state of the environment reflects whether the limits for underlay DSA are being met or not. As such, the state space is defined to have two states where the system is in state  $S_0$  when all CRs transmit with a power level such that none of their respective nearest PN links exceed the limit on relative throughput change, an the system is in state  $S_1$  when any of the PN links nearest to the CRs experiences a relative throughput change that exceeds the underlay DSA limit. It is assumed here that there is a control channel in the SN over which the CRs share a single bit of information indicating the state of their nearest PN link.

**Reward:** The reward function reflects each CR goal to maximize their throughput and is defined as a function of the state and the action taken to transition to a new state, as follows:

$$r_t^{(i)}(a_t, x_t) = \begin{cases} 10^{T_i}, & \text{if environment state is } S_0, \\ 0, & \text{if environment state is } S_1, \end{cases} \quad (1)$$

where  $T_i$  is the throughput on the  $i$ th. SN link. Note that although the reward could have been chosen as a simple function  $r_t^{(i)}(a_t, x_t) = T_i$ , we choose a more complex  $r_t^{(i)}(a_t, x_t) = 10^{T_i}$ . This is because the actions that are being taken consists on transmit power settings, which affect the SINRs in the system and, in turn, SINRs values determine the achievable throughput through a logarithmic relation (consider Shannon's channel capacity). As a result, our chosen reward function provides more distinct reward values for different taken actions. Also, we note that while the above is the reward function proper to our problem solution, in most of the simulation results we used as reward function  $r = 10^{\sum_i T_i}$ , this is, a reward that is a function of the sum throughput in the SN. This is for fair comparison of our proposed solution

against the optimal solution found through exhaustive search. To be optimal, the exhaustive search in the benchmark needs to be for a single global optimum, which is defined as the sum throughput in the SN.

With Q-learning, each agent finds the best policy (mapping from states to actions)  $\pi^*$  that maximizes the expected sum of discounted rewards,

$$V(x, \pi) = \sum_{t=1}^{\infty} \gamma^t E[R_t | \pi, (x_0 = x)], \quad (2)$$

where  $x_0, x$  denotes the initial and the current state,  $\gamma$  is the discount factor and  $R_t$  is the reward for the agent at epoch  $t$ . In the case when the environment model is not known immediately, the expectation of the accumulates discounted rewards can be approximated through the Q-function, using the time difference technique as,

$$Q_{t+1}(x_t, a_t) = Q_t(x_t, a_t) + \alpha_t [R_t + \gamma \max_{a' \in A} [Q_t(x_{t+1}, a') - Q_t(x_t, a_t)]] \quad (3)$$

where  $\alpha_t \in (0, 1)$  is the learning rate. In a table-based Q-learning algorithm, the Q-values  $Q(s, a)$  that are iteratively estimated using (4) by exploring all actions multiple times from all states. However, this approach is impractical in that it involves a very large number of learning steps. The works [2], [3] constitutes a major milestone by introducing the deep Q-networks (DQNs), a new approach to Q-learning that learns faster over large action and state spaces by doing away with the use of a table to update Q values and using instead a deep neural networks as an efficient nonlinear approximator of the Q action-value function. Also, DQN includes a technique known as "experience replay" to improve the learning performance, where at each time step, the experience of each agent with the environment is stored as a tuple  $e_i(t) = (a_i(t), x_i(t), r_i(t), x_i(t+1))$  into a replay memory. Moreover, in DQN each agent utilizes two separate neural networks as Q-network approximators: one as action-value function approximator  $Q_i(x, a; \theta_i)$  and another as target action-value function approximator  $\hat{Q}_i(x, a; \theta_i^-)$ , where  $\theta_i$  and  $\theta_i^-$  denote the parameters (weights) for each neural network. At each learning step, the parameters  $\theta_i$  of each agent's action-value function are updated through mini-batch of random samples of entries from the replay memory. The parameters  $\theta_i$  of the action-value function are updated through a gradient descent backpropagation algorithm using the error function

$$L(\theta_i) = E[(r_i(x, a) + \gamma \max_{\hat{a} \in A} [\hat{Q}_i(\hat{x}, \hat{a}; \theta_i^-)] - Q_i(x, a; \theta_i))^2]. \quad (4)$$

Only every  $c$  learning steps, the parameters  $\theta_i^-$  of the target action-value function are replaced by the updated parameters  $\theta_i$  of the action-value function. This is to damp non-stationarity of the target values, which hampers convergence.

While the above DQN technique, which we'll call as the "standard DQL" approach throughout this paper, has shown significant success in many RL applications, it is a technique for single agent scenarios and as such, shares the positives of single agent Q-learning (e.g. guaranteed convergence to optimal policy as time tends to infinity) and its limitations for multi-agent scenarios as the one at hand in this work. In the present case, by continuously interacting with the environment, the action of any agent (a CR) may affect the

environment of other agents (the transmit power setting of one CR translates into a level of interference to the rest of the SN and the PN), which compounded with a lack of coordination between agents, results in a multi-agent non-stationary environment for which standard DQL would likely not be adequate. This problem of uncoordinated distributed multi-CR resource allocation we are addressing here belongs to a class of notoriously challenging RL problems known as Weakly Acyclic Stochastic Dynamic Games for which there was no known RL algorithm with guaranteed convergence to the optimal policy. However, [1] recently presented a modified general table-based Q-learning algorithm for which almost sure convergence in an asymptotic infinite learning time was proved. We use this work as a basis to present next a novel DQL configuration that shares the positive qualities from standard DQL and inherits the convergence guarantee from the table-based Q-learning algorithm from [1].

As indicated in [1], the main obstacle to convergence in the problem at hand is the presence of multiple active learners interacting through their entanglement over the environment, yielding a non-stationary environment for all learners. Standard DQL already incorporates a mechanism to address non-stationarity of the target action-value function during learning. However, this is not nearly enough for the problem at hand because the non-stationary environment results in "noisy" and non-stationary observations of the reward which, as can be seen in (4), leads to non-convergent behavior in the DQL neural network learning. To address the non-stationary environment issue, [1] introduced the idea of "exploration phases". Now learning occurs over a succession of multiple exploration phases where, during each of them, agents take the action determined by the current policy most of the time and only occasionally (as determined by a random draw with an "experimentation probability") it explores a different action chosen randomly from a uniform distribution. This results in agents experiencing near-stationary environments (with stationarity occasionally broken by exploration of non-current policy actions by other agents), which allows the agents to accurately estimate their action-value function. Coupled with the use of exploration phases, it is necessary to also implement a mechanism for gradual learning of the best policy that does not require coordination between agents. In [1], the technique proposed for this purpose is what is called as a "Best Reply Process with Inertia" mechanism. The basic principle for this mechanism is to select a policy (after each exploration phase) from a set formed from those actions that are associated with a Q-value that is within a tolerance range from the largest Q-value. Inertia in the choice is implemented by keeping the current action with an inertia probability  $\lambda$  (usually larger than 0.5) and choosing one policy from the candidate set with probability  $1 - \lambda$ .

Algorithm 1 shows how all these ideas come together. In the algorithm, lines 10 to 17 comprise an exploration phase, after which lines 18 and 19 perform the best reply process with inertia mechanism. Our implementation of inertia differs from [1] by always choosing a policy from the random draw with probability  $\lambda$ . The tolerance level used in line 18 is also particular to our solution and is calculated as three times the largest moving standard deviation among Q-values. Within

the exploration phase, line 11 shows the choice of action and lines 13 through 16 comprise the implementation of a DQN. In our case, we eliminated the replay memory because it operates counter to the intent of an exploration phase and we eliminated the target action-value neural network, replacing it by an array in memory that stores Q-values.

**Algorithm 1** Uncoordinated Distributed Multi-agent DQN

---

```

1: Set parameters
2:  $\rho \in (0,1)$  : Experimentation probability
3:  $\lambda \in (0,1)$  : Inertia
4:  $\gamma \in (0,1)$  : Discount factor
5: Learning rate  $\alpha_n \in \frac{1}{n^v}$ , where  $v \in (\frac{1}{2}, 1)$ ;
6: Initialize policy  $\pi_0 \in \Pi$  (arbitrary)
7: Sense state  $x_0$ 
8: Initialization of the neural network for action-value function  $Q_i$  with random weights  $\theta_i$ 
9: for  $0 \leq k \leq K$  do
10:   for Iterate  $t = t_k, t_k + 1, \dots, t_{k+1} - 1$  do
11:     (kth. exploration phase)
12:        $a_t = \begin{cases} \pi_k(x_t), & \text{w.p. } 1 - \rho \\ \text{any } a \in A, & \text{w.p. } \rho/|A| \end{cases}$ 
13:     Receive reward  $R_t$ 
14:     Sense state  $x_{t+1}$ ;  $n_t$  = number of visits to  $(x_t, a_t)$ 
15:     Update the state  $x_{t+1}^{(i)}$  and the reward  $R_t^{(i)}$ .
16:     Update parameters  $(\theta)$  of action-value function  $Q(s_t^{(i)}, a_t^{(i)}; \theta_i)$ , mini-batch backpropagation with error function (4)
17:   end for
18:    $\Pi_{k+1}^i = \{\hat{\pi}^i \in \Pi^i : Q_{t_{k+1}}^i(s, \hat{\pi}^i(x)) \geq \max_{v^i} Q_{t_{k+1}}^i(s, v^i) - \delta^i, \text{ for all } s\}$ 
19:    $\pi_{k+1}^i = \begin{cases} \pi_k^i, & \text{w.p. } \lambda \\ \text{any } \pi^i \in \Pi_{k+1}^i, & \text{w.p. } \frac{(1-\lambda)}{|\Pi_{k+1}^i|} \end{cases}$ 
20: end for

```

---

*Remark:* Because our multi-agent DQN maintains all the elements of the table-based Q-learning algorithm from [1] necessary for convergence, we state that our proposed DQL technique achieves almost sure convergence to optimality with learning time tending to infinity, with proof as shown in [1].

#### IV. EXPERIMENTAL RESULTS AND DISCUSSION

##### A. Experimental Setup

We evaluated the proposed multi-agent DQL technique through a series of Monte Carlo simulations with 100 runs. The experimental setup consisted of a PN sharing through underlay DSA a 180 kHz radio spectrum band with an SN formed by CRs implementing the proposed technique. The PN consist of nine access points (APs) organized in a three-by-three rectangular grid, with each AP separated by a distance of 200 m. Of the nine APs, only seven (chosen at random for each Monte Carlo run) are active transmitting over the same spectrum band. Each active provides service to one receiver station located at random within the coverage area of the corresponding AP. The SN is composed of two pairs of CRs with each of the two transmitters located at random

anywhere within the PN three-by-three grid and the two receivers randomly located within 50 m of their corresponding receivers. This setup is intended to broadly model a network of small radio devices (the SN) coexisting through spectrum sharing with an incumbent network (the PN) of larger devices. For underlay spectrum sharing, the limit on relative throughput change on the PN links was set to 5 % in all simulations, where the nearest link to a CR is the one that is received with largest power at the corresponding CR transmitter (as the assessment of its transmission effect on the PN is done by each CR transmitter).

For all channels in both networks, the received signal power,  $P_{Rx}$  undergoes path, penetration and shadowing loss, modeled at a link length of  $d$  km, being equal to  $P_{Rx} = P_{Tx} - 128.1 - 37.6 \log d - 10 - S$ , [13], where all magnitudes are in dBs,  $P_{Tx}$  is the transmit power,  $S$  is the shadowing loss (modeled as a zero-mean Gaussian random variable with 6 dB standard deviation) and the penetration loss is fixed at 10 dB. Also, all channels have AWGN power -130 dBm and they present a delay spread that follows the Pedestrian B typical urban model from [14]. In addition, all transmissions in the PN and SN implement adaptive transmit power and adaptive modulation and coding (AMC). We assumed that PN transmitters can adapt transmit power in the range of -30 and +20 dBm and the SN transmitters select one of fourteen power settings between -10 and 20 dBm (plus no transmission). For simulation purposes, we adopt the AMC scheme defined for LTE (fifteen possible modes combining different channel coding rates and one of QPSK, 16-QAM or 64-QAM modulation scheme), [15]. To avoid edge effects on networks' play field, the three-by-three grid wraps around all its edges.

##### B. Proposed DQL Technique Setup

Following evaluation of multiple configurations we implemented the neural network that learns the action-value function as a five-layer multilayer perceptron (MLP) with input being the sensed environmental state and outputs the Q-values for each possible action. Also, the implemented MLP had three, five and seven neurons in the hidden layers (from input to output). The activation function for all hidden layers was a saturated ReLU (rectified linear unit). The action space for the CRs was defined as the fourteen transmit power levels between -10 and 20 dBm equally spaced by 2.5 dBm, plus no transmission (transmit power zero). Consequently, the output layer was formed by fourteen neurons with a linear activation function (a ReLU activation function yielded marginally better results but hampered the collection of some performance metrics that we are unable to present in this paper due to space limitation). Training for the DQL neural network was done over through backpropagation with the gradient descent algorithm configured (unless otherwise noted in specific experiments) with learning rate equal to 0.01, mini-batch size of 60 training samples consisting of tuples  $\langle \text{current state, next state, action taken, target Q-value} \rangle$ , and epoch (equivalent to one exploration phase) length equal to 60. The neural network weights are initialized with random values uniformly distributed between 0 and 1.

While different simulation experiments explored changes to

different parameter settings, the reference implementation of the proposed DQL technique used the following parameters: number of exploration phases equal to 60, experimentation probability  $\rho = 0.15$ , inertia probability  $\lambda = 0.35$ , update target Q-values every  $c = 30$  training steps.

### C. Results and Analysis

Figs. 1 and 2 compare the RL evolution for, respectively, standard DQL and our proposed approach for the same exemplar system realization. Both figures show the evolution over the training steps of the Q-values associated with each of the actions in state  $S_0$  and the second CR link. Inserts in the figures show zoomed-in portions of the result curves. In the case of using the standard DQL approach, Fig. 1 shows how the non-stationary environment results in “noisy” Q-values which clearly leads to a non-convergent behavior. In this case, the noisy Q-values are because the action exploration of the two CR transmitters results in different pairings of actions from each agent and, consequently, different rewards (and possibly next state) for the same initial state and action. In the particular case of Fig. 1, CR 1 frequently tests actions that transition the system from state  $S_0$  to state  $S_1$ , resulting in all Q-values in CR 2 tending to a value near zero. However, the Q-values do not converge to zero and become noisy because a few of the actions being randomly explored keep the system in state  $S_0$  and yield a reward larger than zero. The end result is that the algorithm is unable to converge and the final policy becomes practically a random choice between four different actions. Importantly, as done for the standard DQL realization, the configuration depicted in Fig. 1 makes use of a separate target action-value set updated every  $c = 60$  training steps, which on the surface could have been considered to provide some level of robustness against the non-stationary environment. However, the important conclusion that is clear from Fig. 1, is that a standard DQL technique may not achieve convergence when used in a multi-agent scenario. In contrast, Fig. 2 depicting the learning evolution for the same CR, in the same network setting and for the same number of training steps, shows how the proposed multi-agent DQL technique succeeds in achieving convergence to the optimal solution. As can be seen in the zoomed-in details of the curve (two levels of details are shown in the figure), the near-stationary environment achieved during exploration phases significantly reduces the “noise” in Q-values (the Q-value corresponding to the active policy presents more noise than the others because it is explored more frequently), yielding low-noise and discernible values. Fig. 1 also shows as a curve with circle markers the tolerance value used during the process of next-policy selection through inertia (the action associated with a Q-value larger than this curve will be a potential next-policy) and how convergence to the optimal policy is occurred in this case near the end of the simulation. This illustrates how in our finite time simulations there may be case where convergence to the optimal policy have not occurred yet. However, as will be seen, we choose parameters so that the performance effect in these occurrences is minimal.

Next, Table I shows the Monte Carlo simulation results. From the simulations we evaluated the ability of the proposed technique to find the optimal solution and address the

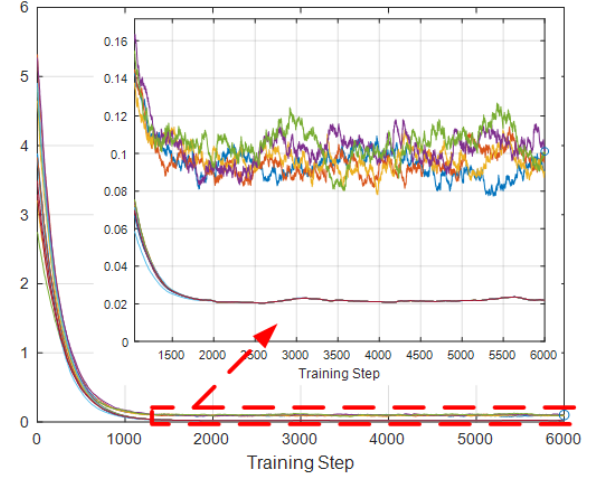


Fig. 1. Evolution of Q-values during multi-agent learning using the standard DQL approach.

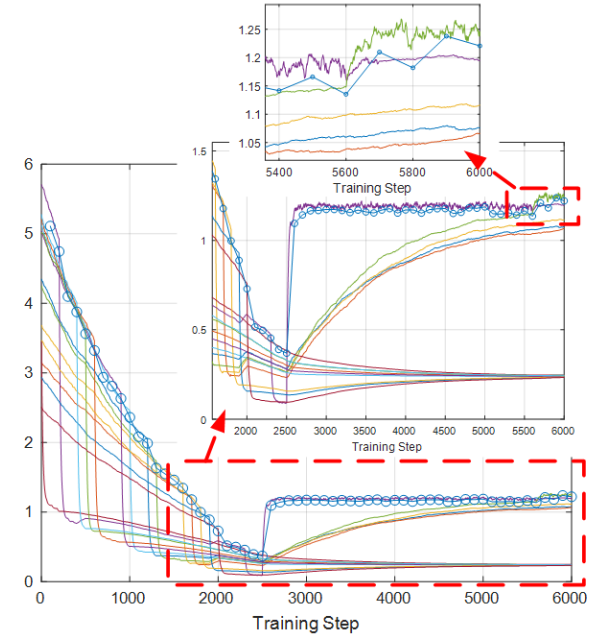


Fig. 2. For the same scenario as in Fig. 1, evolution of Q-values during multi-agent learning using the proposed DQL approach (solution converges to optimal policy).

challenges from the multi-agent resource allocation problem. In the experiments, the optimal solution was calculated as the one resulting from an exhaustive search over all transmit power combinations for both CR links that yields the largest sum throughput in the SN while meeting the limit on relative throughput change on the PN links nearest to each CR transmitter. While the proposed DQL technique will arrive at the optimal solution, this result is guaranteed to happen for the generality of cases when the learning time is allowed to tend to infinity. However, practical deployment in the field and simulation limitations, dictates a finite limit to the learning time. Consequently, we measured the percentage of cases that the proposed algorithm found the optimal policy and also the mean relative absolute difference in the sum throughput achieved by the CR between the optimal solution and the results of our proposed technique. In addition, we measured the mean number of exploration phases needed to reach convergence (counting the cases that do not achieve con-

vergence in the given finite time with the maximum number of exploration phases). The reference parameter settings detailed in subsection IV-B were chosen to provide very small mean relative difference within a reasonable span of time and its results are shown in Table I with the description “Reference setting”.

Description	Mean Relative Difference	Mean Exp. Phases to Converge	Percent Optimal Policy
Reference setting	0.0249	33.62	69
Standard DQL $c = 1$	0.0945	N/A	56
Standard DQL $c = 60$	0.0744	N/A	55
$c = 1$	0.0331	35.18	66
$c = 60$	0.0096	33.42	72
Mini batch size = 120	0.0375	35.6	67
Mini batch size = 30	0.0241	36.35	69
Uncoordinated per-CR reward	0.0411	32.01	70

TABLE I  
RESULTS OF EXPERIMENTS

The experiments described in Table I “Standard DQL  $c = 1$ ” and “Standard DQL  $c = 60$ ” present results for the case of direct application of a standard DQL technique with different settings for the parameter  $c$  that measures the number of training steps in-between refreshing the target Q-values. The results show that in close to half of the cases the algorithm does not converge to the optimal policy. The much larger mean relative difference compared with our proposed technique indicate that many cases will never converge (as was exemplified in Fig. 1. This set of results shows the inadequacy of using the standard DQL approach in the considered multi-agent scenario and Validates our proposed DQL technique.

The rest of experimental results shown in Table I after the standard DQL cases, study the performance of our proposed DQL scheme with different parameter settings. The cases described as “ $c = 1$ ” and “ $c = 60$ ” show that a larger value for the number of steps between refreshing the target Q-values provides some performance improvement. The results described as “Mini batch size = 120” and “Mini batch size = 30” show little performance difference with respect to the mini batch size with respect to the reference setting. In order to compare viz-a-viz to the optimal exhaustive search solutions, all the results presented so far correspond to a DQL implementation where the reward function is a function of the sum throughput across all CRs. However, the actual implementation of the uncoordinated DQL that is of interest would not have the CR sharing their throughput to calculate their sum, and instead, would have each CR calculating a reward that is a function solely of their individual throughput, as in (1). The results for this case are presented in Table I with the “Uncoordinated per-CR reward” description. As can be seen, performance is similar to that of our reference settings (with reward based on the sum throughput in the CRN), confirming the success of our proposed DQL technique, although the mean relative difference is slightly larger in the per-CR reward. This is because of occasional cases where each CR attempts to maximize their own throughput by increasing transmit power with such a coupling between the CRs that the interference on each other results in a sum throughput slightly lower than the optimal. However, we emphasize that the use of

sum throughput as a metric was dictated by the need to define a unique optimal setting to benchmark against, and is not a performance measure that fully corresponds to uncoordinated conditions.

## V. CONCLUSION

In this paper, we presented a novel deep reinforcement learning technique capable of achieving convergence to the optimal solution in the case of uncoordinated interacting multiple-agent CRs. The presented novel DQL technique succeeds in addressing the challenge of a non-stationary multi-agent environment that results from the dynamic interaction between radios through the shared wireless environment in underlay DSA. Simulation results show that under a finite learning time the presented technique finds the optimal policy in nearly 70 % of cases and yields performance within 3% of an exhaustive search optimal solution. We also present a case that shows that standard single-agent deep reinforcement learning may not achieve convergence when used in a non-coordinated, coupled multi-radio scenario.

## REFERENCES

- [1] G. Arslan and S. Yüksel, “Decentralized q-learning for stochastic teams and games,” *IEEE Transactions on Automatic Control*, vol. 62, no. 4, pp. 1545–1558, April 2017.
- [2] V. Mnih, K. Kavukcuoglu, D. Silver, A. A. Rusu *et al.*, “Human-level control through deep reinforcement learning,” *Nature*, vol. 518, no. 7540, p. 529, 2015.
- [3] D. Silver, A. Huang, C. J. Maddison, A. Guez *et al.*, “Mastering the game of go with deep neural networks and tree search,” *Nature*, vol. 529, no. 7587, pp. 484–489, 2016.
- [4] X. Li, J. Fang, W. Cheng, H. Duan, Z. Chen, and H. Li, “Intelligent power control for spectrum sharing in cognitive radios: A deep reinforcement learning approach,” *IEEE Access*, vol. 6, pp. 25 463–25 473, 2018.
- [5] J. Zhu, Y. Song, D. Jiang, and H. Song, “A new deep-q-learning-based transmission scheduling mechanism for the cognitive internet of things,” *IEEE Internet of Things Journal*, 2017.
- [6] Z. Xu, Y. Wang, J. Tang, J. Wang, and M. C. Gursoy, “A deep reinforcement learning based framework for power-efficient resource allocation in cloud rans,” in *Communications (ICC), 2017 IEEE International Conference on*. IEEE, 2017, pp. 1–6.
- [7] Y. He, Z. Zhang, F. R. Yu, N. Zhao, H. Yin, V. C. Leung, and Y. Zhang, “Deep reinforcement learning-based optimization for cache-enabled opportunistic interference alignment wireless networks,” *IEEE Transactions on Vehicular Technology*, vol. 66, no. 11, pp. 10 433–10 445, 2017.
- [8] H. Sun, X. Chen, Q. Shi, M. Hong, X. Fu, and N. D. Sidiropoulos, “Learning to optimize: Training deep neural networks for wireless resource management,” in *Signal Processing Advances in Wireless Communications (SPAWC), 2017 IEEE 18th International Workshop on*. IEEE, 2017, pp. 1–6.
- [9] F. Meng, P. Chen, and L. Wu, “Power allocation in multi-user cellular networks with deep q learning approach,” in *IEEE International Conference on Communications (ICC)*, May 2019, pp. 1–6.
- [10] Y. S. Nasir and D. Guo, “Multi-agent deep reinforcement learning for dynamic power allocation in wireless networks,” *IEEE Journal on Selected Areas in Communications*, vol. 37, no. 10, pp. 2239–2250, Oct 2019.
- [11] Xiaoxin Qiu and K. Chawla, “On the performance of adaptive modulation in cellular systems,” *IEEE Transactions on Communications*, vol. 47, no. 6, pp. 884–895, June 1999.
- [12] F. S. Mohammadi and A. Kwasinski, “Neural network cognitive engine for autonomous and distributed underlay dynamic spectrum access,” *CoRR*, vol. abs/1806.11038, 2018. [Online]. Available: <http://arxiv.org/abs/1806.11038>
- [13] “Further advancements for e-utra physical layer aspects, document 3gpp tr 36.814 v9. 0.0,” *3rd Generation Partnership Project; Technical Specification Group Radio Access Network; E-UTRA*, 2010.
- [14] “Guidelines for evaluation of radio transmission technologies for imt-2000,” *Rec. ITU-R M. 1225*, 1997.

[15] “Physical layer procedures, document 3gpp tr 36.213 v9. 2.0,” *3rd Generation Partnership Project; Technical Specification Group Radio Access Network; E-UTRA*, 2010.